The RhoA GTPase activating protein, DLC2, modulates RhoA activity and hyperalgesia to noxious thermal and inflammatory stimuli

Fred K.C. Chan[1], Stephan S.M. Chung[4], Irene O. Ng[3], Sookja K. Chung[1,2]

[1]Department of Anatomy; [2]Research Center of Heart, Brain, Hormone and Healthy Aging, [3]Department of Pathology, Li Ka Shing Faculty of Medicine, The University of Hong Kong, Hong Kong SAR, China; [4]Division of Science and Technology, United International College, Zhuhai, China

Keywords: Deleted in Liver Cancer 2, pain, nerve conduction velocity, inflammation, hyperalgesia, RhoA, ERK.

Abbreviations: DLC2, deleted in liver cancer 2; RhoGAP, RhoGTPase activating protein; RhoA, Ras homolog gene family member A; ERK, Extracellular signal-regulated kinase.

To whom correspondence should be addressed:
Prof. Sookja K. Chung, Department of Anatomy, 1/F. Laboratory Block, Li Ka Shing Faculty of Medicine,21 Sassoon Road, Hong Kong SAR. Tel: (852) 2819-9172; Fax: (852) 2817-0857; E-mail: skchung@hkucc.hku.hk

Financial support:
This project is funded by CRCG funding, The University of Hong Kong to S.K. Chung

Abstract

Deleted in Liver Cancer 2 (DLC2) is a novel RhoGTPase activating protein (RhoGAP) that regulates RhoA activity. DLC2 is ubiquitously expressed in most tissues, including the brain, spinal cord and peripheral nerves, and is thought to be involved in actin cytoskeletal reorganization. Unlike DLC1-deficient mice, DLC2-deficient mice ($DLC2^{-/-}$) are viable and without gross anatomical abnormalities. Interestingly, $DLC2^{-/-}$ mice exhibit hyperalgesia to noxious thermal stimuli and inflammation-inducing chemicals, such as formalin and acetic acid. There was no difference in the structure or morphology of cutaneous or sural nerves between $DLC2^{+/+}$ and $DLC2^{-/-}$ mice. However, sensory nerve conduction velocity (SNCV) in $DLC2^{-/-}$ mice was significantly higher than that in $DLC2^{+/+}$ mice, whereas motor nerve conduction velocity (MNCV) was not affected. After formalin injection, $DLC2^{-/-}$ mice showed increased RhoA activity in spinal cord and an increased number of phosphorylated ERK1/2-positive cells. The inflammatory hyperalgesia in $DLC2^{-/-}$ mice appeared to be mediated through the activation of RhoA and ERK1/2. Taken together, DLC2 plays a key role in pain modulation during inflammation by suppressing the activation of RhoA and ERK to prevent an exaggerated pain response and that $DLC2^{-/-}$ mice provide a valuable tool for further understanding the regulation of inflammatory pain.

Introduction

Deleted in Liver Cancer 2 (DLC2) is a member of the family of Deleted in Liver Cancer genes; it is also known as Steroidogenic Acute Regulatory protein (StAR)-related lipid transfer (START) Domain-containing protein 13 (DLC2). This gene encodes a protein containing 1,113 amino acids that shares 51% identity and 65% similarity with the amino acid sequence of DLC1 [1]. DLC2 has a sterile alpha (SAM) domain, a START domain and a Rho GTPase activating protein (RhoGAP) domain. An additional functional domain was identified in residues 322-329 as an ATP/GTP-binding site [1].

DLC2 was first thought to be a tumor suppressor gene because it is located on chromosome 13q12.3, a region often deleted in hepatocellular carcinoma (HCC) [2-9]. In addition, DLC2 expression is reduced in 18% of human HCC samples [1]. DLC2 exhibited RhoGAP activity specific for RhoA, which may mediate stress fiber formation [1,10,11]. The increased expression of its RhoGAP domain inhibited the proliferation of breast cancer cells [10] and HepG2 cells [11] by inactivating RhoA. In addition, increased expression of its GAP domain inhibited the migration of HepG2 cells [1,11]. However, one study showed that a DLC2 deficiency did not increase the rate of spontaneous liver tumor formation or diethylnitrosamine (DEN)-induced hepatocarcinogenesis [12].

Activation of RhoA is involved in the initiation and maintenance of inflammatory and neuropathic pain [13,14]. Intraperitoneal injection of the ROCK inhibitor Y27632 in mice produced an anti-nociceptive effect to noxious thermal stimuli and inflammatory agents, such as formalin and acetic acid [14,15]. This was

probably because RhoA and ROCK regulate glutamine and/or acetylcholine release from peripheral nerves [16-18]. Thus, RhoA/ ROCK plays a role in neurotransmitter release from sensory nerves. RhoA is also critical for the regulation of actin cytoskeleton formation during many cellular events. The regulation of the cytoskeleton, especially in nervous tissues, is important for neurite outgrowth, axonal targeting and branching. Although DLC2 is thought to regulate RhoA, its role in actin cytoskeletal organization, the development of nervous tissues and neuropathic pain is not clear.

In this study, we investigated nerve morphology in $DLC2^{-/-}$ mice and their response to noxious thermal stimuli and inflammatory chemicals. We found that there was no significant difference in the structure of the cutaneous and sural nerves compared to that of $DLC2^{+/+}$ mice under normal conditions. In addition, hyperalgesia to heat and inflammation in $DLC2^{-/-}$ mice was associated with increased activity of RhoA and ERK1/2, the signaling molecules involved in hyperalgesia, in the dorsal horn of the spinal cord.

Material and Methods

Animals

Male mice around 9 to 11 week-old were used. Wild type ($DLC2^{+/+}$) and DLC2-deficient ($DLC2^{-/-}$) mice were used. $DLC2^{-/-}$ mice were backcrossed to C57BL/6N for 6 generations. For morphological assessment, $DLC2^{+/+}$ and $DLC2^{-/-}$ mice (N7 backcross to C57BL/6N) were mated with Thy1-YFP mice, which had yellowish-green fluorescent protein in the sensory and motor neurons (31). All mice were maintained in a 12/12 hr light/dark cycle with food and water *ad libitum*.

Animal experiments were carried out following the guidelines set forth by the Committee on the Use of Live Animals in Teaching and Research at The University of Hong Kong.

Reverse-transcription PCR (RT-PCR)

For semi-quantitative RT-PCR analysis, total RNA was prepared from mouse tissues using TRI reagent. First strand cDNA was synthesized from 1μg of total RNA using SuperScript^{TM} (Invitrogen) reverse transcriptase. DLC2 mRNA and GAPDH were amplified by following primers: for DLC2 gene, a forward primer (5'-TGTGCTGGCAGGGACGGC) and a reverse primer (5'-TGCCAATGTGCTGTGACTTTGCAG) were used; for GAPDH, a forward primer (5'- CATCACCATCTTCCAGGA) and a reverse primer (5'-CAGATCCACGACGGACA) were used. The annealing temperature of the PCR was 55□ with 25 cycles. After PCR, 10 μl of PCR reaction mixture was applied to electrophoresis. The gel was stained and exposed to UV to visualize the band and captured by Gel Doc XR (Bio-Rad). The intensity of the expected band was quantified by ImageJ (NIH). The intensity of the bands in different lane was normalized with level of GAPDH, which served as a loading control.

In situ hybridization

A pair of specific primers for amplification of DLC2 riboprobe (forward primer: 5'- GGTCTGCTCTATTCACA and reverse primer: 5'-TGCAAAGTCACAGCACATTGGCA) was designed using the free online software Primer 3 based on the published sequence of DLC2 (NM_146258.1). PCR fragments of DLC2 were generated from mouse brain cDNA, and cloned into the pBluescript II SK+ vector. One μg purified linearized DNA plasmid served as

template for RNA probe synthesis by *in vitro* RNA transcription with DIG labeling. The antisense or sense RNA probes were synthesized with T7 or T3 RNA polymerase, respectively, in transcription buffer (400mM Tris-HCL pH8.0, 60mM $MgCl_2$, 100mM Dithiothreitol, 20mM spermidine) and DIG RNA labeling mix (Genius). The chromogenic reaction was carried out using BM purple in AP buffer.

Hot plate test and tail flick test

The animals were tested for their response to heat stimulus [19]. Mice were placed in the bottom of a 4 L glass beaker, which was incubated in a water-bath kept at 55^{o}C, and the responsive time required for the mice to lick and lift their rear paws or jump was determined. The maximum time for heat stimulus was 30 seconds to avoid tissue damage of the footpad. For the tail flick test, the tail of mouse was immersed in water maintained at 52.5℃ and the time for the mouse to flick their tail was recorded as withdrawal latency. The maximum time of heat stimulus was 30 seconds to avoid tissue damage of the tail.

Formalin test

A volume of 20 µl of 1% formalin solution was injected through a fine-gauge needle subcutaneously into the dorsal surface of one hind paw. The length time engaged in licking and biting of the hind paw was recorded in the first 10 minutes and then between the 20 minutes to 30 minutes time points. The first 10 minutes or Phase I measured the acute pain response to the chemical. The period between 20 to 30 minutes is the Phase II pain response to inflammation.

Abdominal constriction tests

Mice were injected intraperitoneally with 10 ml/kg of 0.6% acetic acid or 10

ml/kg of 12 mg/ml Magnesium sulfate as control. They were then placed in an observation cage and the numbers of abdominal constrictions within the first 5 minutes or within 30 minutes were recorded.

Open field test

Mice were placed in a 240 x 240 mm transparent plastic box for assessment. A 100x100 mm arena at the center of the box was marked. The movement was recorded by a video camera that was connected to a computer for tracking and recording. The data were analyzed with EthoVision (Noldus) software, which revealed the total time the mouse was in motion, total distance traveled, velocity, and time spent in the center arena or margin of the arena.

Porsolt swim test

The cylinder with 100 mm diameter was filled with water to at least 100 mm height. Day 1 was a training session. Mice were placed in water-filled cylinder for 6 minutes. Testing sessions were performed on Day 2. Mice were placed in a water-filled cylinder for 6 minutes, and its movement was recorded by a video camera and analyzed by EthoVision (Noldus) software as above.

Measurement of nerve conduction velocity

The nerve conduction velocity was measured in mice with 9 to 11 week-old according to the protocol mentioned previously [20,21]. Briefly, mice were anesthetized with Ketamine (100 mg/kg)/ Xylazine (10 mg/kg) and the sciatic nerve were stimulated (5-10 V, 0.05 ms single square-wave pulses) proximally with platinum needle electrodes (Grass, Quincy, MA). Compound muscle action potentials were recorded from the ipsilateral foot between digit 2 and 3. Afterwards, the length of sciatic

nerve was measured. The first compound action potential from individual stimulation was used for the measurement of motor latency, while the second one was used for the measurement of sensory latency. NCV was calculated by difference of latencies between stimulation sites (Latency of M-wave (Notch) - Latency of M-wave (Ankle)) over the length of sciatic nerve [22].

Protein analysis using Western blotting

Lumbar 4 to 5 spinal cords were dissected from mice 5 minutes, 30 minutes or 1 day post-formalin injection into their footpads. Spinal cords were rinsed with ice-cold PBS and separated longitudinally through the anterior median fissure to the posterior median sulcus. The half of spinal cord, which received the injection of PBS or formalin, was defined as the ipsilateral side, whereas the uninjected side was defined as contralateral side. Each half of spinal cord was lysed separately by sonication in lysis buffer (50 mM Tris HCl pH7.4; 1% NP-40; 0.25% Na-deoxycholate; 150 mM NaCl; 1 mM PMSF) and 50μg of protein extract was subjected to 12% SDS-polyacrylamide gel electrophoresis (PAGE). The gel was transferred to a polyvinylidene difluoride membrane (Hybond-P, GE healthcare). The membrane was blotted with anti-pERK (1:1000, cell signaling), and then rescreened with anti-total ERK (1:1000, cell signaling) and then finally blotted with anti-GAPDH (1:1000, abcam). The immunoreactivity was detected with enhanced chemiluminescence according to the procedure provide by GE healthcare.

Rhotekin binding assay

Tissues were lysed by sonication in lysis buffer (50 mM Tris HCl pH7.4; 1% NP-40; 0.25% Na-deoxycholate; 150 mM NaCl; 1 mM PMSF). Each sample was sonicated twice for 30 seconds. The lysates were spun at 13,000 rpm for 2 minutes at 4^{o}C.

The amount of protein was measured by BioRad protein assay. The lysates were diluted into 1μg/μl. 500 μl of diluted lysates were used for RhoA-pull down assay. 10 μl of cleaned agarose beads (Glutathione Sepharose 4B, GE Healthcare) were added to each sample and incubated for 1 hour at 4^{o}C. The lysates were transfer to new tubes and 50 μg of GST-RBD (GST fusion protein containing RhoA-binding domain of Rhotekin) bead was added into each sample and incubated with shaking for 1 hour at 4^{o}C. The supernatant was removed and the beads were washed in washing buffer for three times. Bound proteins were fractionated on 12% SDS/PAGE and detected with polyclonal antibody for RhoA (1:1000, Santa Cruz Biotechnology). Total tissue lysate was also analyzed with anti-RhoA antibody as a loading control. The level of active RhoA was determined after normalization with the total RhoA present in the tissue lysates.

In vivo quantification of cutaneous nerve in live animals

The method of quantification of cutaneous nerves was according to the protocol mentioned previously [23]. Briefly, animals were anesthetized with Ketamine (100mg/kg)/ Xylazone (10mg/kg). Hair on a defined area of the leg was removed and cleaned by PBS. Three squares of 4mm x 4mm were marked on both legs: mid-calf, mid-thigh and one in between those two areas. The YFP positive small cutaneous fibers were quantitated under fluorescence stereomicroscope. The density of all primary and secondary YFP positive nerve fibers in these areas of the legs was expressed as average number of YFP positive fiber per 100mm^2 (# fibers/100mm). The observer was blinded to the genotype of experimental animals. The image of YFP positive nerve fibers were captured by the Leica DC500 camera attached to the fluorescence stereomicroscope and processed with Leica IM 50 software.

Histological and Immunocytochemical analysis

Footpad skins of mice were harvested and embedded in OCT. The skin samples were sectioned at 60 μm and were mounted on poly-L-lysine coated glass slide, and then the sections were dried on the drier at 37 ^{o}C for 30 minutes. The sections were washed with 1xPBS for 5minutes and post-fixed with 4% PFA for 5minutes. After fixation, the sections were rinsed with 1xPBS for 5minutes. The slides were mounted with FluorSave^{TM} (Merck Ltd.) and coverslip. Five regions of skin section were chosen and the images of these five regions were taken by using Confocol microscope (Zeiss 510-Meta). The criteria of counting small free ending nerve was followed the methods describe in Lauria et al [24]

Lumbar 4 to 5 spinal cords were dissected from mice 5 minutes, 30 minutes or 1 day after they received the 1% formalin injection into their footpads. The spinal cords were fixed in 4% paraformaldehyde for 2 hours at room temperature (RT) and then perfused with 20% sucrose overnight at 4 ^{o}C. The cryopreserved spinal cords were sectioned at 20 μm using cryostat (CM3000, Leica) and then mounted on poly-L-lysine coated glass slides.

Spinal cord sections were submerged in 4% paraformaldehyde (PFA) for 20 minutes at RT and then washed 3 times in phosphate-buffered saline (PBS) for 5 minutes. Diluted primary antibodies (anti-phosphorylated ERK1/2 (1:100, Cell signaling) was applied and incubated at 4^{o}C for 16-18 hours The sections were then washed 3 times with 1xPBS for 5 minutes. For pERK staining, diluted secondary antibodies (goat anti-rabbit) were applied to each section and were incubated at room temperature in the dark for 60 minutes. After secondary antibody incubation, slides were washed with 1x PBS for 5 minutes. The ABC complex was added to each section and

incubated for 30 minutes at RT. Slides were then washed with 1x PBS for 5 minutes. The sections were then incubated in daminobenzidine (DAB) for 2 minutes and then rinsed in 1x PBS. After washing off the antibody, images were captured using fluorescent microscope (Leica). The numbers of pERK-positive neurons in the superficial laminae (I–II) quantitated according to the method of mentioned in previous reports [25,26].

Morphometric analysis of sural nerves

Sural nerves of $DLC2^{+/+}$ and $DLC2^{-/-}$ mice were harvested and were fixed in primary fixative overnight at 4 ^{o}C. Then, the tissues were rinsed in 0.1 M phosphate buffer 3 times for 5 minutes. The tissues were post-fixed in 1% Osmium tetroxide for 2 hours at 4 ^{o}C. After post-fixation, the tissues were rinsed in 0.1 M phosphate buffer 3 times for 5 minutes. After washing, the tissues were dehydrated in ascending ethanol series. After dehydration, tissues were infiltrated with propylene oxide, and propylene oxide: Epon (50:50) for 1 hour. Tissues were transferred to 100% Epon for overnight on rotator, embedded in epon and polymerized in 60 ^{o}C oven for 72 hours. The 1 μm thick transverse sections of nerves were cut using Ultracut (Reichert-Jung, Leica) mounted on TESPA coated glass slides and counter-stained with toludine blue. The photomicrographs of sural nerves were taken at a magnification of 1,000X using a computer-assisted image analyzing system (SPOT). Fascicular area, feret diameter, myelinated fiber number and size were analysed and measured by ImageJ (NIH).

Statistical analysis

All data were expressed as means ± SEM. Statistical analysis was performed by

Student *t-test*, Mann Whitney or One-way ANOVA. P values 0.05 were considered statistically significant.

Results

DLC2 mRNA is expressed in brain, spinal cord and sciatic nerve tissue

To analyze the role of DLC2 in the neural control of pain, gene expression in brain, spinal cord and peripheral nerve tissue was analyzed using semi-quantitative RT-PCR. As shown in Figure 1 A, DLC2 mRNA was present in each tissue and as expected, absent in the corresponding tissues from $DLC2^{-/-}$ mice. Within the brain, DLC2 expression was high in the cortex, cerebellum, hippocampus, and brainstem and low in the midbrain and olfactory bulb. In situ hybridization confirmed that DLC2 mRNA is localized in neurons of $DLC2^{+/+}$ mice in the above-mentioned regions, and expression was not detected in these areas in $DLC2^{-/-}$ mice. (Fig. 1 B).

Increased RhoA activity in nervous tissues of DLC2-deficient mice

The role of DLC2 as a RhoGAP specific for RhoA was established using cell lines [11,27]. However, this function has not been confirmed in animal tissues. Therefore, RhoA activity in the brain and the peripheral nerves of $DLC2^{+/+}$ and $DLC2^{-/-}$ mice was assessed using the Rhotekin binding assay [11,27]. Significant differences in RhoA activity were not found in the brain tissue of $DLC2^{+/+}$ and $DLC2^{-/-}$ mice (N=5) (Fig. 1 C-ii). Interestingly, RhoA activity was significantly increased in the peripheral nerves of $DLC2^{-/-}$ mice compared to that of $DLC2^{+/+}$ mice (Fig. 1 C-iv).

DLC2-deficient mice experience more severe hyperalgesia

Because RhoA has been implicated in pain sensation, and the regions of the brain

in which DLC2 was highly expressed have been linked to pain processing pathways [28-32], we determined whether DLC2 is involved in pain sensation. We compared the response of 9-11-week-old $DLC2^{+/+}$ and $DLC2^{-/-}$ mice to noxious thermal stimuli and inflammatory chemical-induced pain. In the hot plate and tail flick tests, DLC2-deficient mice showed shorter paw and tail withdrawal latencies than the $DLC2^{+/+}$ mice, suggesting that the former were more sensitive to painful thermal stimuli (Fig. 2 a, b).

An injection of 1% formalin to the right hind paw causes the mouse to lick, bite its paw, and flinch its leg. Such behavioral responses occur within 10 minutes (Phase I) and within 20-30 minutes (Phase II) of the formalin injection. Phase I is also referred to as the acute phase, whereas the Phase II is often referred to as inflammation-induced pain phase. During Phase I, the frequency of licking and flinching of $DLC2^{-/-}$ mice was not different from that of $DLC2^{+/+}$ mice. However, $DLC2^{-/-}$ mice showed a significantly more intense Phase II pain response than the $DLC2^{+/+}$ mice. These mice spent more time biting, licking or flinching their right hind paw (Fig. 2 d). The enhanced response to inflammatory pain in the formalin-injected $DLC2^{-/-}$ mice was not due to more severe inflammation, as both $DLC2^{-/-}$ and $DLC2^{+/+}$ mice showed a similar degree of swelling in the right hindpaw (data not shown).

An intraperitoneal injection of acetic acid and magnesium sulfate produces acute inflammatory pain and acute non-inflammatory, prostaglandin-independent pain, respectively [33]. In response to the acetic acid injection, $DLC2^{-/-}$ mice showed significantly more abdominal constriction than $DLC2^{+/+}$ mice (Fig. 2 e). In contrast, injection of magnesium sulfate resulted in a similar response in the $DLC2^{-/-}$ and

$DLC2^{+/+}$ mice (Fig. 2 f).

DLC2-deficient mice have normal locomotor activity and do not exhibit anxiety or depressive behaviors

DLC2 expression was analyzed in the hippocampus and the zona incerta, which are involved in locomotor activity, anxiety, depressive-like behavior and pain modulation. In addition, anxiety is one of the potential components of the pain response [34]. Therefore, we examined $DLC2^{-/-}$ mice to determine whether they have any abnormalities in locomotive function, anxiety or depressive behavior.

In the open field test, which examines general exploratory and locomotor activity, no significant differences in the total duration of locomotor activity and total distance traveled within one hour were observed between $DLC2^{-/-}$ and $DLC2^{+/+}$ mice, suggesting that the loss of DLC2 expression did not affect habituation (Fig. 2 g, h). In addition, no significant difference in the moving velocity was observed between the mice, suggesting that locomotor activity was not affected by the DLC2-deficiency (Fig. 2 i). Furthermore, no differences in the time spent in the center of the test field were observed, suggesting that each genotype had a normal level of anxiety (Fig. 2 j).

In the Porsolt swim test, which is designed to reveal depression-like behavior [33,35], $DLC2^{-/-}$ mice behaved similar to the $DLC2^{+/+}$ mice in terms of the amount of struggling time and the amount of time spent floating (Fig. 2 k). An increase in the floating time is indicative of depression because mice stop trying to get out of the water.

DLC2-deficient mice show increased sensory nerve conduction velocity, but the

sural nerve morphology appears normal

Sensory (SNCV) and motor nerve conduction velocity (MNCV) in the sciatic nerve of 9-11-week-old $DLC2^{+/+}$ and $DLC2^{-/-}$ mice was determined as described in the Materials and Methods. The $DLC2^{-/-}$ mice MNCV appeared normal (Fig. 2 l); however, the SNCV was increased compared to that of the $DLC2^{+/+}$ mice (Fig. 2 m).

Because only the SNCV was affected in $DLC2^{-/-}$ mice, the sensory nerve morphology (i.e., sural nerve) of the $DLC2^{+/+}$ and $DLC2^{-/-}$ mice was examined (Fig. 3 a, b). Semi-thin (1 μm) sections of the sural nerve were prepared, and morphometric analysis of the myelinated fibers was performed because these fibers are likely to affect nerve conduction velocity. These data showed no difference in the fascicular area and minimum feret diameter (Fig. 3 c, d), the number and density of myelinated fibers (Fig. 3 e, f), axon diameter (Fig. 3 g, h), and thickness of myelin (Fig. 3 i) between $DLC2^{-/-}$ and $DLC2^{+/+}$ mice. In addition, the area of un-myelinated fibers was not significantly different between $DLC2^{+/+}$ and $DLC2^{-/-}$ mice (Fig. 3 j). Taken together, these data suggest that the loss of DLC2 does not affect sural nerve morphology.

The number of cutaneous nerve fibers is not different between $DLC2^{+/+}$ and $DLC2^{-/-}$ mice

A transgene that labels nerve fibers with a yellowish-green fluorescent protein (YFP) [23] was introduced into $DLC2^{+/+}$ and $DLC2^{-/-}$ mice to facilitate non-invasive visualization of cutaneous nerve fibers. Both small and large YFP-labeled fibers in the skin can be visualized under the fluorescent microscope (Fig. 3 k). Large nerve fibers were found in the dermis parallel to the skin surface (red arrow, Fig. 3k-i). The small fibers (white arrowhead, Fig. 3 k-i) in the epidermal layer perpendicular to

the skin surface were cutaneous nerves. The nerves that branched out from the large fibers were termed primary fibers (Fig. 3 k-ii, white arrowhead), whereas those bifurcating from the primary fibers (Fig. 3 k-iii, white arrow) were termed secondary fibers. Non-invasive microscopic visualization was unable to distinguish between myelinated and un-myelinated fibers.

We quantified the cutaneous nerve fiber density in three regions of the thigh in 9-11-week-old DLC2$^{+/+}$ YFP and DLC2$^{-/-}$ YFP mice [23]. As shown in Figure 3 l, there was no significant difference in the primary and secondary cutaneous nerve fibers between DLC2$^{+/+}$ and DLC2$^{-/-}$ mice. The cutaneous nerve fiber density within the epidermis and perpendicular to the dermis in five regions of the footpad skin was also examined and also showed no difference between the DLC2$^{+/+}$ and DLC2$^{-/-}$ mice (Fig. 3 m, n).

RhoA activity in spinal cord of DLC2-deficient mice is increased 30 minutes after a formalin injection

To determine whether RhoA was involved in the Phase II hyperalgesia response in DLC2$^{-/-}$ mice, RhoA activity in the spinal cord 30 minutes after the formalin injection was determined. In DLC2$^{+/+}$ mice, the RhoA activity was not different between the ipsilateral (same side as formalin injection) and contralateral (opposite side of formalin injection) side of the L1-S1 spinal cord (Fig. 4). In DLC2$^{-/-}$ mice, a significant increase in RhoA activity was observed in the ipsilateral side of spinal cord compared to the contralateral side (Fig. 4 b).

The number of phosphorylated ERK1/2-positive cells in spinal dorsal horn is increased

Phosphorylation of ERK in the spinal dorsal horn is thought to play an important role in the inflammatory pain response [36]. To determine whether ERK1/2 is involved in hyperalgesia in DLC2$^{-/-}$ mice, spinal cords were dissected 5 minutes and 30 minutes after a formalin injection and were stained with antibodies against phosphorylated ERK1/2 (pERK1/2).

In naïve DLC2$^{+/+}$ and DLC2$^{-/-}$ mice, the number of pERK1/2-positive cells in the superficial layer of spinal dorsal horn was not significantly different (Fig. 5a). The number of pERK1/2-positive cells in the ipsilateral dorsal horn of DLC2$^{+/+}$ mice was significantly increased 5 minutes after the injection in comparison to the contralateral side (Fig. 5 a-i and 5a-ii). The number of pERK1/2-positive cells in the ipsilateral side of DLC2$^{-/-}$ mice was also significantly higher in comparison to the contralateral side (Fig. 5 a-iii and 5 a-iv); however, the degree of increase was much more than that of DLC2$^{+/+}$ mice (Fig. 5 a-i, a-iii and Fig. 5 d-i). At 30 minutes after the formalin injection, the number of pERK1/2-positive cells in the superficial spinal dorsal horn was reduced in both the contralateral and ipsilateral sides in the DLC2$^{+/+}$ and DLC2$^{-/-}$ mice (Fig. 5 c and d-ii), and no significant difference in the number of pERK1/2-positive cells was observed.

Western blot analysis confirmed that the pERK1/2 level in the ipsilateral spinal cord of DLC2$^{-/-}$ mice was significantly higher than that of the DLC2$^{+/+}$ mice (Fig. 5 d-iii and d-iv). However, the difference in pERK1/2 expression between the contralateral and ipsilateral spinal cord of the DLC2$^{+/+}$ and the difference of pERK1/2 expression between the contralateral and ipsilateral spinal cord of DLC2$^{-/-}$ mice was not observed in the quantitative Western blot histogram.

Discussion

Loss of DLC2 does not affect locomotor activity, anxiety and depression

In this report, we showed that DLC2 null mice were more sensitive to noxious thermal stimuli and chemically induced inflammatory pain. DLC2 is a newly identified RhoGAP specific for RhoA [1,11]. Several RhoGAPs are thought to be involved in neuronal morphogenesis. Oligophrenin-1 appears to play a role in neurite outgrowth and the regulation of synaptic connectivity [37]. p250GAP, which is a RhoGAP for RhoA and Cdc42, is enriched in the NMDA receptor complex and regulates dendritic spine structure in an NMDA receptor-dependent manner [38]. DLC1 is also a RhoGAP specific for RhoA and Cdc42 [39], and it is thought to be involved in neural tube development. DLC1 null mice die *in utero* due to defects in neural tube development [40]. One of the RhoGAPs, p190GAP, is involved in axon guidance and fasciculation [41]. Interestingly, DLC2 null mice appeared normal with no obvious abnormality in the nervous tissues. Their locomotor activity appeared normal without exhibiting any signs of anxiety-like or depression-like behavior in the open field test and Porsolt swim test, respectively. The morphology of the cutaneous nerves, such as the sural nerve, appeared normal.

More severe hyperalgesia is observed in DLC2-deficient mice

Interestingly, DLC2$^{-/-}$ mice were more sensitive to noxious thermal stimuli and inflammatory pain. An hyperalgesic response to noxious thermal stimuli was observed in the hot plate and tail flick tests. In addition, an hyperalgesic response to inflammatory pain was determined by quantifying the Phase II response during a formalin test. The abdominal constriction response to an inflammatory agent was also determined. DLC2$^{-/-}$ mice were hypersensitive to acetic acid-induced

(inflammatory) pain, whereas they exhibited a normal response to magnesium sulfate-induced (non-inflammatory acute) pain. Hyperalgesia to inflammatory pain in DLC2$^{-/-}$ mice was not due to increased inflammation in the injected footpads, as the swelling of the injected footpads was not significantly different from that of the DLC2$^{+/+}$ mice (data not shown). Taken together, these observations indicate that DLC2 is involved in the modulation of pain sensation. DLC2 expression was present in several regions of the brain that are involved in pain modulation, including the hippocampus CA1 region [31], dentate gyrus [42] and zona incerta [43].

SNCV is increased in DLC2$^{-/-}$ mice

The DLC2$^{-/-}$ mice showed a normal MNCV, although the SNCV was increased compared to that of the DLC2$^{+/+}$ mice. The SNCV measured in this study was the conduction velocity of a H-reflex, which runs from the sensory nerves to the spinal cord and back to the motor nerves [44]. A faster SNCV may thus contribute to a shorter withdrawal latency in the hot plate test and the tail flick test. Increased RhoA activity in the peripheral nerves of DLC2$^{-/-}$ mice may also contribute to the hypersensitivity to thermal stimuli, as the activation of RhoA and ROCK induce neurotransmitter release through a reorganization of the actin cytoskeleton [14].

The increased SNCV in DLC2$^{-/-}$ mice was not associated with a noticeable change in the structure of the sural nerves. The fascicular area, the number of myelinated fibers and axon diameter were similar in both the DLC2$^{+/+}$ and DLC2$^{-/-}$ mice. Unfortunately, the resolution of the sural nerve semi-thin sections was not sufficient to reveal the morphology of the un-myelinated fibers. The area of un-myelinated fibers in the sural nerves was determined by deducing the fascicular area by the area of the myelinated fibers. The area of the un-myelinated fibers in the

sural sections was not significantly different between DLC2$^{+/+}$ and DLC2$^{-/-}$ mice. Our data suggest that DLC2$^{-/-}$ mice have normal sural nerve morphology and myelination.

In addition to the nerve structure, the post-synaptic release of nitrite oxide (NO) and its subsequent diffusion play an important role in synaptic plasticity and long-term potentiation [45]. ROCK regulates NO release through the stimulation of prostaglandin E2 (PGE2) [46]. Determining NADPH-diaphorase and nNOS activity in the DLC2$^{-/-}$ mice would shed light on the role of RhoA in nerve conduction velocity. Moreover, RhoA activation induces the release of neurotransmitters such as glutamate through the reorganization of the actin cytoskeleton at the cell periphery by activating ROCK and myristoylated alanine-rich C-kinase substrate (MARCKS) [17]. The increase in pre-synaptic RhoA activity also induced acetylcholine release in *C. elegans* through an unknown mechanism [18]. Therefore, increased SNCV in DLC2$^{-/-}$ mice may be the result of altered synaptic connectivity and function, although further studies are required to support this hypothesis.

RhoA activity is increased in the spinal cord of DLC2$^{-/-}$ mice after a formalin injection

The injection of formalin into the rodent hindpaw produces two distinct phases of nociceptive behavior. These two pain phases involve different physiological mechanisms. The Phase I pain response occurs during the chemical activation of primary afferent nociceptors at the injection sites, whereas the Phase II pain response is the result of factors released from local inflammation at the injection site. In this study, the DLC2$^{-/-}$ mice displayed a hyperalgesic Phase II response after the formalin injection, indicating that DLC2 may modulate inflammatory pain. This phenotype

was confirmed by the acetic acid abdominal contraction test (Fig. 2e), which is another inflammatory pain test.

Hyperalgesia induced by inflammatory pain in DLC2$^{-/-}$ mice may involve RhoA. A dramatic increase in RhoA activity was observed in the ipsilateral spinal cord 30 minutes after the formalin injection. It is well known that the activation of RhoA and its effector, ROCK, is related to spinal nociceptive transmission [14,47-49] and that the inhibition of ROCK attenuates inflammatory and neuropathic pain [13,47]. In addition, a recent paper showed that the RhoA/ROCK pathway is also involved in thermal hyperalgesia in diabetic mice [50]. Furthermore, the activation of RhoA and ROCK is related to spinal nociceptive transmission [14,47-49], and the inhibition of ROCK attenuates inflammatory and neuropathic pain [13,47], whereas the activation of RhoA by the injection of LPA induces hyperalgesia and allodynia [13]. The injection of H-1152, a ROCK inhibitor, significantly reduced the Phase II pain behavior resulting from a formalin injection by attenuating the phosphorylation of MARCKS in the superficial dorsal horn of the spinal cord [14]. Therefore, RhoA and ROCK are important regulators of inflammatory pain, and the de-regulation of RhoA may influence the inflammatory pain response.

The *in vivo* function of the DLC2-RhoGAP domain has not been fully determined. *In vitro*, the DLC2-RhoGAP domain showed Rho-GAP activity for RhoA and CDC42 [1], and the over-expression of DLC2 inhibited RhoA activity, resulting in the reduction of actin stress fiber formation [11,51] and suggesting that DLC2 predominately regulates RhoA. Because DLC2 is a negative regulator of RhoA, it may be involved in the suppression of RhoA activity. These data suggest the activity of RhoA may be negatively regulated by DLC2 in pain modulation.

ERK1/2 signaling may affect DLC2-induced hyperalgesia

ERK1/2 activation is involved in the inflammatory pain response but does not affect basal pain sensitivity [26]. Increased ERK1/2 activation was detected after Complete Freund's Adjuvant (CFA)-induced inflammatory pain [26]. In addition, the inhibition of pERK1/2 attenuates inflammatory [25,36,52], heat and mechanical pain hypersensitivity [26]. In this study, we observed an increase in the number of pERK1/2-positive cells in the ipsilateral dorsal horn of the spinal cord (L4 and L5) of $DLC2^{-/-}$ mice 5 minutes after a formalin injection, which is similar to a previous report [25]. The activity of ERK1/2 in both sides of the spinal cord was increased in $DLC2^{-/-}$ mice compared to $DLC2^{+/+}$ mice.

In contrast to the immunocytochemical data, the quantitative Western blot analysis did not show an increase in pERK1/2 in the ipsilateral spinal cord compared to the contralateral side in the $DLC2^{+/+}$ mice 5 minutes after a formalin injection. Western blot analysis showed that pERK1/2 was increased in both the contralateral and ipsilateral sides of the spinal cord in $DLC2^{-/-}$ mice compared to $DLC2^{+/+}$ mice 5 minutes after a formalin injection. Nevertheless, an increase in pERK1/2 in the ipsilateral dorsal horn of the spinal cord in $DLC2^{-/-}$ mice was observed compared to $DLC2^{+/+}$ mice 5 minutes after a formalin injection.

The activation of ERK1/2 peaks 5 minutes after stimulation and then decays 30 to 60 minutes after stimulation [25,26,53]. It is not yet clear whether ERK1/2 activation occurs 5 minutes after a formalin injection, but the hyperalgesic effects were observed during Phase II, 20-30 minutes post injection. Some studies suggest that ERK1/2 is involved in the central sensitization to acute noxious stimuli [26] and

increased excitability of spinal neurons through the phosphorylation of the A-type potassium channel, Kv4.2 [54]. In addition, ERK1/2 induces transcriptional changes in the spinal cord. pERK1/2 translocates to the nucleus and phosphorylates the transcription factor cAMP element-binding protein (CREB) and induces transcription via CREB kinase [55-57]. Moreover, the activation of ERK has been shown to induce NK1, which plays an important role in inflammatory pain hypersensitivity [58,59], and the expression of prodynorphin, which is involved in inflammation-induced enhanced excitability and expanded dorsal horn neuronal receptive fields [60,61] after the induction of inflammatory pain [26]. Therefore, the activation of ERK may contribute to acute inflammatory hyperalgesia through post-translational and -transcriptional regulation.

Recently, increasing evidences have suggested that RhoA regulates ERK1/2 signaling directly or through the regulation of MEK [62-64], although evidence for a direct link between RhoA and ERK1/2 activation in nervous tissues has not yet been determined. In this study, ERK1/2 activity in the ipsilateral spinal cord of DLC2$^{-/-}$ mice peaked 5 minutes after the formalin injection, whereas RhoA in the ipsilateral spinal cord of DLC2$^{-/-}$ mice was significantly activated 30 minutes post injection, after Phase II. These data suggest that the induction of pERK1/2 in DLC2$^{-/-}$ mice during inflammatory pain may be independent of RhoA activation. Whereas, a recent study showed that DLC2 up-regulated pERK1/2 in HepG2 through Raf-1-ERK1/2-p70S6K pathway [27], suggesting that further investigation is necessary to reveal the underlying mechanism involving DLC2, RhoA and ERK1/2 in pain perception.

Taken together, we have shown that DLC2 has RhoGAP activity for RhoA in

nervous tissue. Loss of DLC2 led to the activation of RhoA and hyperalgesia after painful stimuli, such as formalin injection. Concomitantly, increased ERK1/2 phosphorylation was also observed in the ipsilateral side of spinal cord of DLC2$^{-/-}$ mice after injecting the animals with the inflammatory agent formalin (Fig. 6). The ERK activation also induced hypersensitivity to pain through the up-regulation of various downstream effectors and an increase in neuronal excitability in the spinal cord [54]. Furthermore, ROCK activation downstream of RhoA may also contribute to hypersensitivity to pain by the phosphorylation of MARCKS and increased glutamate release. However, the precise mechanism involving DLC2, RhoA and ERK1/2 has not yet been identified. Therefore, further investigation is necessary to determine the detailed mechanism of DLC2 involvement in inflammatory pain.

References

1 Ching YP, Wong CM, Chan SF, Leung TH, Ng DC, Jin DY, Ng IO: Deleted in liver cancer (DLC) 2 encodes a RhoGAP protein with growth suppressor function and is underexpressed in hepatocellular carcinoma. J Biol Chem 2003;278:10824-10830.

2 Laurent-Puig P, Legoix P, Bluteau O, Belghiti J, Franco D, Binot F, Monges G, Thomas G, Bioulac-Sage P, Zucman-Rossi J: Genetic alterations associated with hepatocellular carcinomas define distinct pathways of hepatocarcinogenesis. Gastroenterology 2001;120:1763-1773.

3 Piao Z, Park C, Park JH, Kim H: Allelotype analysis of hepatocellular carcinoma. Int J Cancer 1998;75:29-33.

4 Kuroki T, Fujiwara Y, Nakamori S, Imaoka S, Kanematsu T, Nakamura Y: Evidence for the presence of two tumour-suppressor genes for hepatocellular carcinoma on chromosome 13q. Br J Cancer 1995;72:383-385.

5 Nagai H, Pineau P, Tiollais P, Buendia MA, Dejean A: Comprehensive allelotyping of human hepatocellular carcinoma. Oncogene 1997;14:2927-2933.

6 Lin YW, Sheu JC, Huang GT, Lee HS, Chen CH, Wang JT, Lee PH, Lu FJ: Chromosomal abnormality in hepatocellular carcinoma by comparative genomic hybridisation in Taiwan. Eur J Cancer 1999;35:652-658.

7 Zondervan PE, Wink J, Alers JC, JN IJ, Schalm SW, de Man RA, van Dekken H: Molecular cytogenetic evaluation of virus-associated and non-viral hepatocellular carcinoma: analysis of 26 carcinomas and 12 concurrent dysplasias. J Pathol 2000;192:207-215.

8 Wong N, Lai P, Pang E, Leung TW, Lau JW, Johnson PJ: A comprehensive karyotypic study on human hepatocellular carcinoma by spectral karyotyping. Hepatology 2000;32:1060-1068.

9 Wang G, Zhao Y, Liu X, Wang L, Wu C, Zhang W, Liu W, Zhang P, Cong W, Zhu Y, Zhang L, Chen S, Wan D, Zhao X, Huang W, Gu J: Allelic loss and gain, but not genomic instability, as the major somatic mutation in primary hepatocellular carcinoma. Genes Chromosomes Cancer 2001;31:221-227.

10 Nagaraja GM, Kandpal RP: Chromosome 13q12 encoded Rho GTPase activating protein suppresses growth of breast carcinoma cells, and yeast two-hybrid screen shows its interaction with several proteins. Biochem Biophys Res Commun 2004;313:654-665.

11 Leung TH, Ching YP, Yam JW, Wong CM, Yau TO, Jin DY, Ng IO: Deleted in liver cancer 2 (DLC2) suppresses cell transformation by means of inhibition of RhoA activity. Proc Natl Acad Sci U S A 2005;102:15207-15212.

12 Yau TO, Leung THY, Lam SGS, Cheung OF, Khong PL, Lam AKM, Chung SK, Ng IOL: Deleted in Liver Cancer 2 (DLC2) Was Dispensable for Development and Its

Deficiency Did Not Aggravate Hepatocarcinogenesis. PLoS One 2009
13 Inoue M, Rashid MH, Fujita R, Contos JJ, Chun J, Ueda H: Initiation of neuropathic pain requires lysophosphatidic acid receptor signaling. Nat Med 2004;10:712-718.
14 Tatsumi S, Mabuchi T, Katano T, Matsumura S, Abe T, Hidaka H, Suzuki M, Sasaki Y, Minami T, Ito S: Involvement of Rho-kinase in inflammatory and neuropathic pain through phosphorylation of myristoylated alanine-rich C-kinase substrate (MARCKS). Neuroscience 2005;131:491-498.
15 Büyükafşa K, Yalçın I, Kurt AH, Tiftik RN, Sahan-Firat S, Aksu F: Rho-kinase inhibitor, Y-27632, has an antinociceptive effect in mice. European Journal of Pharmacology 2006;541:49-52.
16 Büyükafşa K, Levent A: Involvement of Rho/Rho-kinase signalling in the contractile activity and acetylcholine release in the mouse gastric fundus. Biochemical and Biophysical Research Communications 2003;303:777-781.
17 Sasaki Y: New aspects of neurotransmitter release and exocytosis: Rho-kinase-dependent myristoylated alanine-rich C-kinase substrate phosphorylation and regulation of neurofilament structure in neuronal cells. J Pharmacol Sci 2003;93:35-40.
18 McMullan R, Hiley E, Morrison P, Nurrish SJ: Rho is a presynaptic activator of neurotransmitter release at pre-existing synapses in C. elegans. Genes Dev 2006;20:65-76.
19 Crawley JN: What's Wrong With My Mouse? Behavioral Phenotyping of Transgenic and Knockout Mice. New York, Wiley-Liss, 2000.
20 Song Z, Fu DT, Chan YS, Leung S, Chung SS, Chung SK: Transgenic mice overexpressing aldose reductase in Schwann cells show more severe nerve conduction velocity deficit and oxidative stress under hyperglycemic stress. Mol Cell Neurosci 2003;23:638-647.
21 Ho EC, Lam KS, Chen YS, Yip JC, Arvindakshan M, Yamagishi S, Yagihashi S, Oates PJ, Ellery CA, Chung SS, Chung SK: Aldose reductase-deficient mice are protected from delayed motor nerve conduction velocity, increased c-Jun NH2-terminal kinase activation, depletion of reduced glutathione, increased superoxide accumulation, and DNA damage. Diabetes 2006;55:1946-1953.
22 De Koning P, Gispen WH: Org.2766 improves functional and electrophysiological aspects of regenerating sciatic nerve in the rat: Peptides, 1987, 8, pp 415-422.
23 Chen YS, Chung SS, Chung SK: Noninvasive monitoring of diabetes-induced cutaneous nerve fiber loss and hypoalgesia in thy1-YFP transgenic mice. Diabetes 2005;54:3112-3118.

24 Lauria G, Cornblath DR, Johansson O, McArthur JC, Mellgren SI, Nolano M, Rosenberg N, Sommer C: EFNS guidelines on the use of skin biopsy in the diagnosis of peripheral neuropathy. Eur J Neurol 2005;12:747-758.
25 Ji RR, Baba H, Brenner GJ, Woolf CJ: Nociceptive-specific activation of ERK in spinal neurons contributes to pain hypersensitivity. Nat Neurosci 1999;2:1114-1119.
26 Ji RR, Befort K, Brenner GJ, Woolf CJ: ERK MAP kinase activation in superficial spinal cord neurons induces prodynorphin and NK-1 upregulation and contributes to persistent inflammatory pain hypersensitivity. J Neurosci 2002;22:478-485.
27 Leung TH, Yam JW, Chan LK, Ching YP, Ng IO: Deleted in liver cancer 2 suppresses cell growth via the regulation of the Raf-1-ERK1/2-p70S6K signalling pathway. Liver Int 2010;30:1315-1323.
28 Tanaka H, Yoshida T, Miyamoto N, Motoike T, Kurosu H, Shibata K, Yamanaka A, Williams SC, Richardson JA, Tsujino N, Garry MG, Lerner MR, King DS, O'Dowd BF, Sakurai T, Yanagisawa M: Characterization of a family of endogenous neuropeptide ligands for the G protein-coupled receptors GPR7 and GPR8. Proc Natl Acad Sci U S A 2003;100:6251-6256.
29 Lee DK, Nguyen T, Porter CA, Cheng R, George SR, O'Dowd BF: Two related G protein-coupled receptors: the distribution of GPR7 in rat brain and the absence of GPR8 in rodents. Brain Res Mol Brain Res 1999;71:96-103.
30 Neugebauer V, Li W, Bird GC, Han JS: The amygdala and persistent pain. Neuroscientist 2004;10:221-234.
31 Khanna S, Chang LS, Jiang F, Koh HC: Nociception-driven decreased induction of Fos protein in ventral hippocampus field CA1 of the rat. Brain Res 2004;1004:167-176.
32 Lanteri-Minet M, Isnardon P, de Pommery J, Menetrey D: Spinal and hindbrain structures involved in visceroception and visceronociception as revealed by the expression of Fos, Jun and Krox-24 proteins. Neuroscience 1993;55:737-753.
33 Mogil JS, Wilson SG, Bon K, Lee SE, Chung K, Raber P, Pieper JO, Hain HS, Belknap JK, Hubert L, Elmer GI, Chung JM, Devor M: Heritability of nociception II. 'Types' of nociception revealed by genetic correlation analysis. Pain 1999;80:83-93.
34 Kelly MA, Beuckmann CT, Williams SC, Sinton CM, Motoike T, Richardson JA, Hammer RE, Garry MG, Yanagisawa M: Neuropeptide B-deficient mice demonstrate hyperalgesia in response to inflammatory pain. Proc Natl Acad Sci U S A 2005;102:9942-9947.
35 Gyires K, Torma Z: The use of the writhing test in mice for screening different types of analgesics. Arch Int Pharmacodyn Ther 1984;267:131-140.
36 Karim F, Hu HJ, Adwanikar H, Kaplan D, Gereau RWt: Impaired inflammatory

pain and thermal hyperalgesia in mice expressing neuron-specific dominant negative mitogen activated protein kinase kinase (MEK). Mol Pain 2006;2:2.
37 Ramakers GJ: Rho proteins and the cellular mechanisms of mental retardation. Am J Med Genet 2000;94:367-371.
38 Nakazawa T, Watabe AM, Tezuka T, Yoshida Y, Yokoyama K, Umemori H, Inoue A, Okabe S, Manabe T, Yamamoto T: p250GAP, a novel brain-enriched GTPase-activating protein for Rho family GTPases, is involved in the N-methyl-d-aspartate receptor signaling. Mol Biol Cell 2003;14:2921-2934.
39 Wong CM, Lee JM, Ching YP, Jin DY, Ng IO: Genetic and epigenetic alterations of DLC-1 gene in hepatocellular carcinoma. Cancer Res 2003;63:7646-7651.
40 Durkin ME, Avner MR, Huh CG, Yuan BZ, Thorgeirsson SS, Popescu NC: DLC-1, a Rho GTPase-activating protein with tumor suppressor function, is essential for embryonic development. FEBS Lett 2005;579:1191-1196.
41 Brouns MR, Matheson SF, Settleman J: p190 RhoGAP is the principal Src substrate in brain and regulates axon outgrowth, guidance and fasciculation. Nat Cell Biol 2001;3:361-367.
42 Soleimannejad E, Semnanian S, Fathollahi Y, Naghdi N: Microinjection of ritanserin into the dorsal hippocampal CA1 and dentate gyrus decrease nociceptive behavior in adult male rat. Behav Brain Res 2006;168:221-225.
43 Masri R, Quiton RL, Lucas JM, Murray PD, Thompson SM, Keller A: Zona incerta: a role in central pain. J Neurophysiol 2009;102:181-191.
44 Tucker KJ, Tuncer M, Türker KS: A review of the H-reflex and M-wave in the human triceps surae. Human Movement Science 2005;24:667-688.
45 Gally JA, Montague PR, Reeke GN, Jr., Edelman GM: The NO hypothesis: possible effects of a short-lived, rapidly diffusible signal in the development and function of the nervous system. Proc Natl Acad Sci U S A 1990;87:3547-3551.
46 Matsumura S, Abe T, Mabuchi T, Katano T, Takagi K, Okuda-Ashitaka E, Tatsumi S, Nakai Y, Hidaka H, Suzuki M, Sasaki Y, Minami T, Ito S: Rho-kinase mediates spinal nitric oxide formation by prostaglandin E2 via EP3 subtype. Biochem Biophys Res Commun 2005;338:550-557.
47 Ye X, Inoue M, Ueda H: Botulinum toxin C3 inhibits hyperalgesia in mice with partial sciatic nerve injury. Jpn J Pharmacol 2000;83:161-163.
48 Buyukafsar K, Yalcin I, Kurt AH, Tiftik RN, Sahan-Firat S, Aksu F: Rho-kinase inhibitor, Y-27632, has an antinociceptive effect in mice. Eur J Pharmacol 2006;541:49-52.
49 Ohsawa M, Mutoh J, Hisa H: Mevalonate sensitizes the nociceptive transmission in the mouse spinal cord. Pain 2008;134:285-292.

50 Ohsawa M, Aasato M, Hayashi SS, Kamei J: RhoA/Rho kinase pathway contributes to the pathogenesis of thermal hyperalgesia in diabetic mice. Pain 2011;152:114-122.
51 Kawai K, Kiyota M, Seike J, Deki Y, Yagisawa H: START-GAP3/DLC3 is a GAP for RhoA and Cdc42 and is localized in focal adhesions regulating cell morphology. Biochem Biophys Res Commun 2007;364:783-789.
52 Ji RR: Peripheral and central mechanisms of inflammatory pain, with emphasis on MAP kinases. Curr Drug Targets Inflamm Allergy 2004;3:299-303.
53 Sasagawa S, Ozaki Y-i, Fujita K, Kuroda S: Prediction and validation of the distinct dynamics of transient and sustained ERK activation. Nat Cell Biol 2005;7:365-373.
54 Morozov A, Muzzio IA, Bourtchouladze R, Van-Strien N, Lapidus K, Yin D, Winder DG, Adams JP, Sweatt JD, Kandel ER: Rap1 couples cAMP signaling to a distinct pool of p42/44MAPK regulating excitability, synaptic plasticity, learning, and memory. Neuron 2003;39:309-325.
55 Impey S, Obrietan K, Wong ST, Poser S, Yano S, Wayman G, Deloulme JC, Chan G, Storm DR: Cross talk between ERK and PKA is required for Ca2+ stimulation of CREB-dependent transcription and ERK nuclear translocation. Neuron 1998;21:869-883.
56 Obrietan K, Impey S, Smith D, Athos J, Storm DR: Circadian regulation of cAMP response element-mediated gene expression in the suprachiasmatic nuclei. J Biol Chem 1999;274:17748-17756.
57 Xing J, Ginty DD, Greenberg ME: Coupling of the RAS-MAPK pathway to gene activation by RSK2, a growth factor-regulated CREB kinase. Science 1996;273:959-963.
58 Abbadie C, Trafton J, Liu H, Mantyh PW, Basbaum AI: Inflammation increases the distribution of dorsal horn neurons that internalize the neurokinin-1 receptor in response to noxious and non-noxious stimulation. J Neurosci 1997;17:8049-8060.
59 McCarson KE, Krause JE: NK-1 and NK-3 type tachykinin receptor mRNA expression in the rat spinal cord dorsal horn is increased during adjuvant or formalin-induced nociception. J Neurosci 1994;14:712-720.
60 Dubner R, Ruda MA: Activity-dependent neuronal plasticity following tissue injury and inflammation. Trends Neurosci 1992;15:96-103.
61 Hylden JL, Nahin RL, Traub RJ, Dubner R: Effects of spinal kappa-opioid receptor agonists on the responsiveness of nociceptive superficial dorsal horn neurons. Pain 1991;44:187-193.
62 Stahle M, Veit C, Bachfischer U, Schierling K, Skripczynski B, Hall A, Gierschik P, Giehl K: Mechanisms in LPA-induced tumor cell migration: critical role

of phosphorylated ERK. J Cell Sci 2003;116:3835-3846.
63 Zhu S, Korzh V, Gong Z, Low BC: RhoA prevents apoptosis during zebrafish embryogenesis through activation of Mek/Erk pathway. Oncogene 2008;27:1580-1589.
64 Li H, Ung CY, Ma XH, Li BW, Low BC, Cao ZW, Chen YZ: Simulation of crosstalk between small GTPase RhoA and EGFR-ERK signaling pathway via MEKK1. Bioinformatics 2009;25:358-364.

Legends for figures:

Figure 1. Disruption of the DLC2 gene result in a loss of DLC2 mRNA expression determined by semi-quantitative RT-PCR and visualized by *in-situ* hybridization: **A.** Semi-quantitative RT-PCR showed the expression of DLC2 in brain, spinal cord and sciatic nerves in brain (i), sciatic nerve (ii) and spinal cord (iii) of $DLC2^{+/+}$ mice and was absent in $DLC2^{-/-}$ mice. Photomicrographs showed DLC2 mRNA in various brain regions (N=3) (iv) and it was absent in all region of brain of $DLC2^{-/-}$ mice. The expression of DLC2 mRNA was normalized with GAPDH. Cx, Cortex; Ce, Cerebellum; Hi, Hippocampus; M, Middle part of brain; O, Olfactory bulb; Bs, Brainstem. Data are showed as mean ± S.E.M. **B.** Photomicrographs showed DLC2 mRNA expression in whole brain of $DLC2^{+/+}$ (a) and was absent in brain of $DLC2^{-/-}$ mice (b). (Scale bar: 1mm). High magnification photomicrographs showed DLC2 mRNA expression in brain of mice in region of hippocampus ($DLC2^{+/+}$: c,d and $DLC2^{-/-}$: e,f) and thalamus ($DLC2^{+/+}$: g,h and $DLC2^{-/-}$: i,j) (Scale bar: 10μm). CA1, field CA1 hippocampus; CA2, field CA2 hippocampus; CA3, field CA3 hippocampuses; DG, dentate gyrus; CP, choroids plexus; DLG, dorsal lateral geniculate nuclei; PGMC, pre-geniculate nuclei magnocel ; SubG, subgeniculate nuclei ; ZIV, zona incerta ventral. Photomicrographs showed mRNA localization in DRG of $DLC2^{+/+}$ (k) and $DLC2^{-/-}$ mice (l). (Scale bar: 10μm). **C.** Micrographs showed Western blotting of RhoA pull-down assay from brain (i) and peripheral nerves (including brachial plexus and sciatic nerves) (ii) of $DLC2^{+/+}$ and $DLC2^{-/-}$ mice. Upper band showed RhoA level after pulling down (Rho-GTP) and lower band showing total RhoA in protein extract. Histogram showed the quantification of active RhoA in brain (iii) and peripheral nerves (iv) of $DLC2^{+/+}$ and $DLC2^{-/-}$ mice which was normalized by total RhoA in the extract (N=5). Data are showed as mean ± S.E.M. * <0.05 by Mann-Whitney test. Y-axis represented ratio of RhoA-GTP/Total RhoA.

Figure 2. Pain perception tests in $DLC2^{+/+}$ and $DLC2^{-/-}$ mice:
(a) Histogram showing hotplate test in $DLC2^{+/+}$ and $DLC2^{-/-}$ mice of 9-11 weeks old (N=15). (b) Histogram showing Tail flick test in $DLC2^{+/+}$ and $DLC2^{-/-}$ mice (N=13). (c) Histogram showing formalin-induced pain response in acute pain phase, which is 10 minutes after injection. (d) Histogram showing formalin induced pain response in inflammatory pain phase, which is the 20^{th} to 30^{th} minute after injection. PBS control (N=3) group; experimental group (N=10). (e) Scatter plot showing the number of abdominal constrictions within 30 minutes after injection of 0.6% acetic acid i.p, $DLC2^{+/+}$ mice (N=9) and $DLC2^{-/-}$ mice (N=11). (f) Scatter plot showing the

number of abdominal constrictions within 5 minutes after injection of 120mg/kg $MgSO_4$, (N=14). (g) Graph showed the time spent in traveling in $DLC2^{+/+}$ and $DLC2^{-/-}$ mice of 9-11 weeks old in open field test (N=7). (h) Histograms showing the total time spent in traveling during 60 minutes in 9-11 weeks old mice (N=7). (i) Histograms showed velocity of mice during 60 minutes in 9-11 weeks old mice (N=7). (j) Histograms showed the total time spent in central arena in open field test in 9-11 weeks old mice (N=7). (k) Histograms showed time spent in immobile in Porsolt swim test. Histograms showing the motor (l) sensory (m) nerve conduction velocity in 9-11 weeks old of $DLC2^{+/+}$ and $DLC2^{-/-}$ mice (N=10). Data are showed as mean ± S.E.M. * <0.05, **<0.01 by Mann-Whitney test.

Figure 3. Morphological study in nerves of $DLC2^{-/-}$ mice: Morphological analysis of sural nerve in $DLC2^{+/+}$ and $DLC2^{-/-}$ mice: Semi-thin section of sural nerve of $DLC2^{+/+}$ (a) and $DLC2^{-/-}$ (b) mice (Scale bar: 10μm) were stained with toludine blue. (c) Histogram showing mean of fascicular area of sural nerve. (d) Histogram showing mean of fascicular diameter of sural nerve. (e) Histogram showing mean of total number of myelinated fibers. (f) Histogram showing mean of myelinated fiber density of sural nerve. (g) Histogram showing diameter of myelinated fiber in sural nerve. (h) Histogram showing area diameter of axon. (i) Histogram showing thickness of myelin in myelinated fiber. Y-axis represented thickness of myelin (μm). (j) Histogram showing the area of unmyelinated fiber. Data are showed as mean ± S.E.M. N=5 in each group of animals. (k) Photomicrographs showing the cutaneous YFP fiber in the leg (i). The insert on the right hand panel (ii,iii) showed the magnified image of boxed area (1,2) The white arrow heads pointed to the primary small fiber, and the white arrows pointed to the secondary small fibers. The red arrow pointed to large nerve fibers in the dermis parallel to skin surface. (l) Histogram showing the cutaneous small fiber density of $DLC2^{+/+}$ and $DLC2^{-/-}$ mice. N=7 in each group of animals. Each column is shown as mean ± SEM. (Scale bar: 100μm). (m) Photomicrographs showing the cutaneous YFP small fiber in the skin section of plantar surface of $DLC2^{+/+}$ /Thy1.2-YFP (1) and $DLC2^{-/-}$ /Thy1.2-YFP (2) mice. The white arrows pointed to the representative free ending cutaneous YFP small fiber. (n) Histogram showing the cutaneous small fiber density of $DLC2^{+/+}$ and $DLC2^{-/-}$ mice. Data are shown as mean ± SEM. N=7 in each group of animals. k.l.: keratin layer; ep.: epidermis, d.: dermis. (Scale bar: 50μm).

Figure 4. RhoA activity assay in DLC2$^{+/+}$ and DLC2$^{-/-}$ mice 30 minutes after formalin injection: (a) Photograph showing Western blotting result of RhoA activity. Upper panel showing the level of active RhoA (RhoA-GTP), middle panel showing the level of total RhoA in lysate and lower panel showing the level of GAPDH in total lysate. Con.: contralateral side of spinal cord; Ips: ipsilateral side of spinal cord. (b) Histogram showing quantification of RhoA activity after formalin injection. The activity RhoA was normalized with total RhoA in lysate. Sample size was 8 in each group. Data expressed as mean ± S.E.M. *<0.05 by 1-way ANOVA.

Figure 5. Phosphorylated ERK immunoreactivity in superficial dorsal horn of spinal cord after 1% formalin injection: a-c. Representative micrographs showed the superficial dorsal horn of spinal cord in DLC2$^{+/+}$ (i, ii) and DLC2$^{-/-}$ (iii, iv) mice with pERK1/2 immunocytochemical staining in naïve condition (a), 5 minutes post-formalin injection (b) and 30 minutes post-formalin injection (c). No obvious pERK1/2 stained cells found on the both side of superficial dorsal horn in DLC2$^{+/+}$ (a-i and a-ii) and DLC2$^{-/-}$ (a-iii and a-iv) mice in naïve condition. The number of pERK positive cells (indicated with arrow in magnified images of (b-i) and (b-iii)) was quantified in ipsilateral (b-i, b.iii; c-i, c.iii) and contralateral (b-ii, b-iv; c-ii, c-iv) side of dorsal horn spinal cord. **d.** Histogram showing the quantitation of pERK positive cells in superficial dorsal horn 5 minutes (d-i) or 30 minutes (d-ii) after 1% formalin injection. Sample size was 4 in each group. (Scale bar: 100μm). **d.iii.** Photomicrograph showing the Western blotting of pERK in spinal cord 5 minutes after formalin injection. **d-iv**. Histograms showing the ratio of pERK1/2 (both band of pERK1/2) to total ERK1/2. Data were shown as mean ± S.E.M. *<0.05; **<0.01, ***<0.001 by One-way ANOVA; # <0.05 by Student's t-test).

Figure 6. Schematic diagram of the possible role of DLC2 and its downstream effectors: DLC2 involves in the regulation of inflammatory pain perception via RhoA and its two possible downstream effectors, ROCK and ERK. Dotted lines indicate the effects between components, but the nature of their interaction remains to be investigated.

Figure 1.

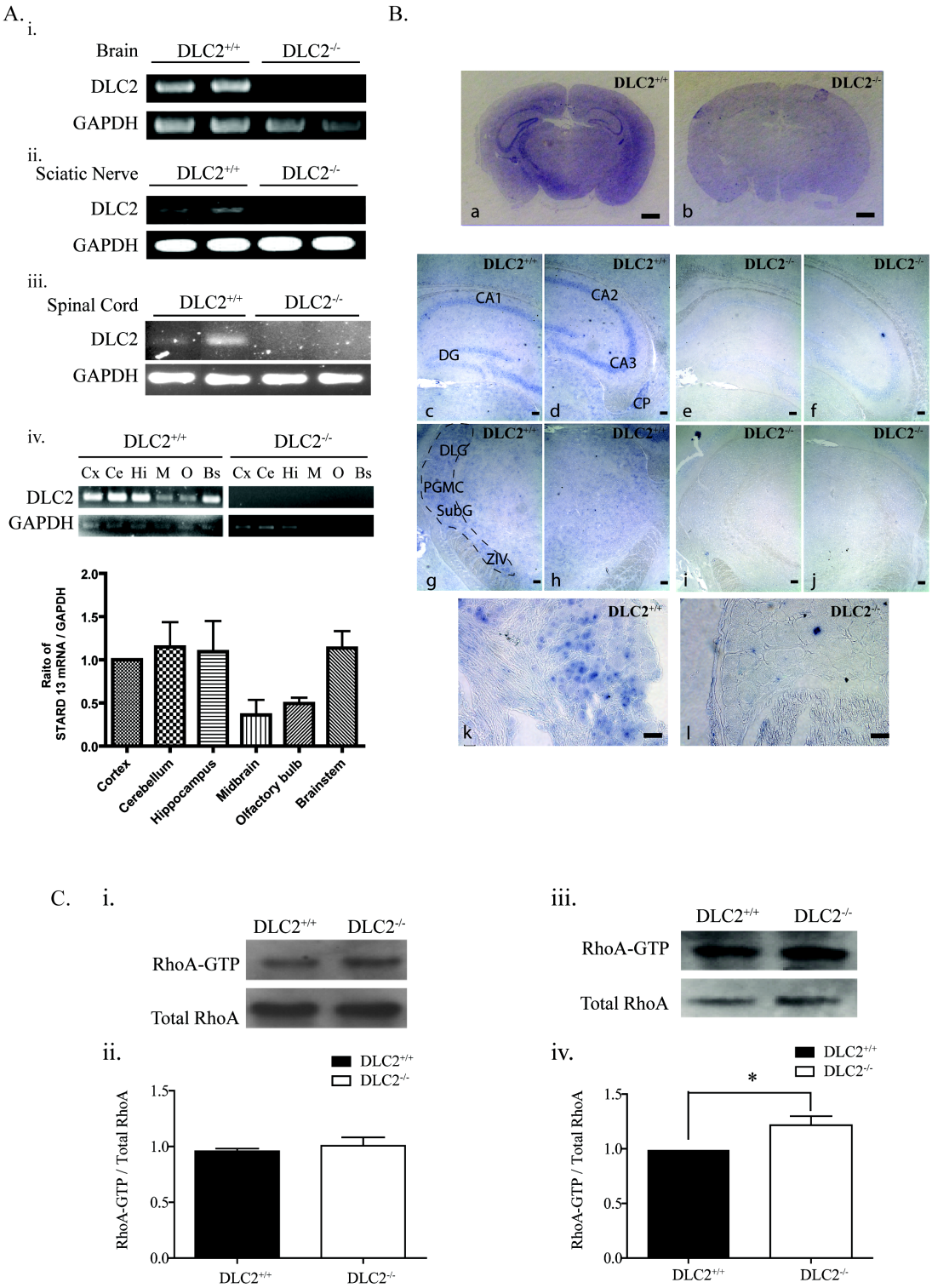
A.
i.
Brain
DLC2+/+
DLC2-/-
DLC2
GAPDH
ii.
Sciatic Nerve
iii.
Spinal Cord
iv.
Cx Ce Hi M O Bs
Raito of STARD 13 mRNA / GAPDH
Cortex
Cerebellum
Hippocampus
Midbrain
Olfactory bulb
Brainstem
B.
CA1
CA2
CA3
DG
CP
DLG
PGMC
SubG
ZIV
C.
i.
RhoA-GTP
Total RhoA
ii.
RhoA-GTP / Total RhoA
iii.
iv.
*

Figure 2.

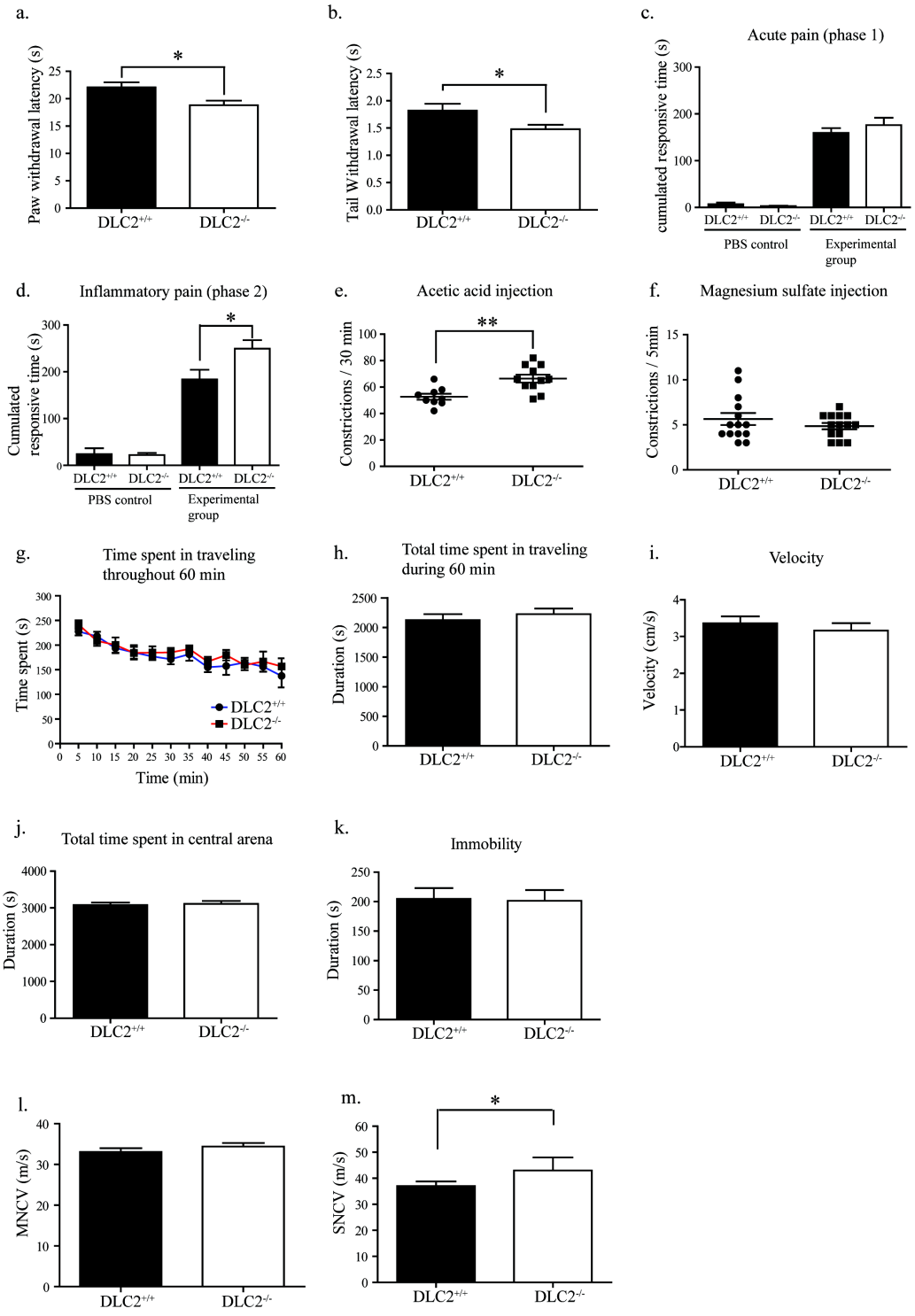
a.
Paw withdrawal latency (s)
DLC2+/+
DLC2-/-
b.
Tail Withdrawal latency (s)
c.
Acute pain (phase 1)
cumulated responsive time (s)
PBS control
Experimental group
d.
Inflammatory pain (phase 2)
Cumulated responsive time (s)
e.
Acetic acid injection
Constrictions / 30 min
f.
Magnesium sulfate injection
Constrictions / 5min
g.
Time spent in traveling throughout 60 min
Time spent (s)
Time (min)
h.
Total time spent in traveling during 60 min
Duration (s)
i.
Velocity
Velocity (cm/s)
j.
Total time spent in central arena
k.
Immobility
l.
MNCV (m/s)
m.
SNCV (m/s)

Figure 3.

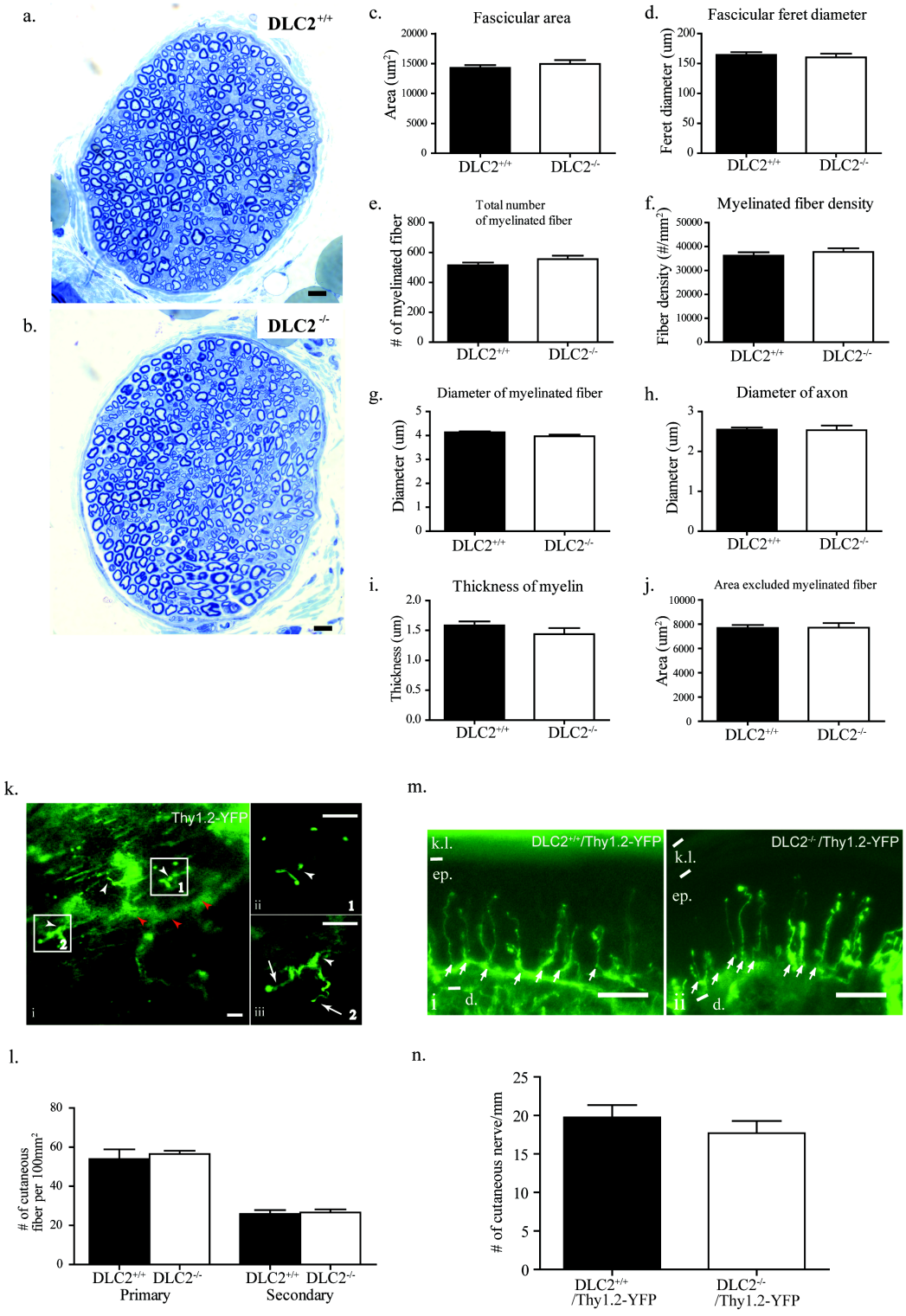
a.
DLC2+/+
b.
DLC2-/-
c.
Fascicular area
Area (um2)
20000
15000
10000
5000
0
DLC2+/+
DLC2-/-
d.
Fascicular feret diameter
Feret diameter (um)
200
150
100
50
0
DLC2+/+
DLC2-/-
e.
Total number of myelinated fiber
# of myelinated fiber
800
600
400
200
0
DLC2+/+
DLC2-/-
f.
Myelinated fiber density
Fiber density (#/mm2)
50000
40000
30000
20000
10000
0
DLC2+/+
DLC2-/-
g.
Diameter of myelinated fiber
Diameter (um)
5
4
3
2
1
0
DLC2+/+
DLC2-/-
h.
Diameter of axon
Diameter (um)
3
2
1
0
DLC2+/+
DLC2-/-
i.
Thickness of myelin
Thickness (um)
2.0
1.5
1.0
0.5
0.0
DLC2+/+
DLC2-/-
j.
Area excluded myelinated fiber
Area (um2)
10000
8000
6000
4000
2000
0
DLC2+/+
DLC2-/-
k.
Thy1.2-YFP
1
2
i
ii
iii
m.
k.l.
ep.
DLC2+/+/Thy1.2-YFP
DLC2-/-/Thy1.2-YFP
d.
i
ii
l.
# of cutaneous fiber per 100mm2
80
60
40
20
0
DLC2+/+ DLC2-/-
Primary
DLC2+/+ DLC2-/-
Secondary
n.
# of cutaneous nerve/mm
25
20
15
10
5
0
DLC2+/+ /Thy1.2-YFP
DLC2-/- /Thy1.2-YFP

Figure 4.

a.

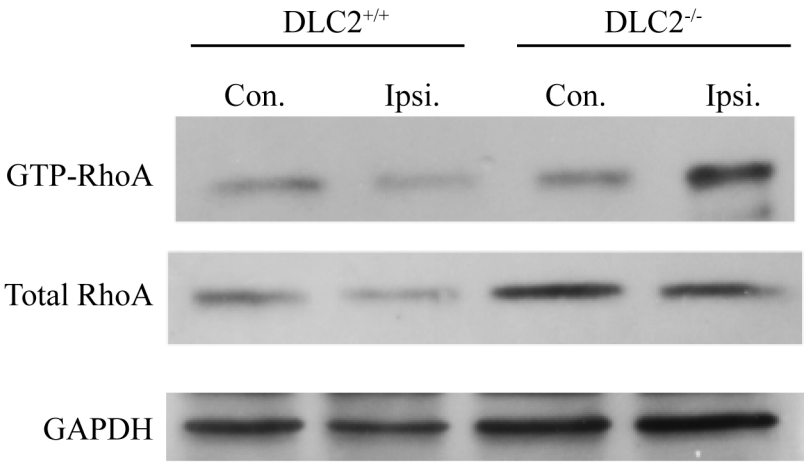
DLC2+/+
DLC2-/-
Con.
Ipsi.
Con.
Ipsi.
GTP-RhoA
Total RhoA
GAPDH

b.

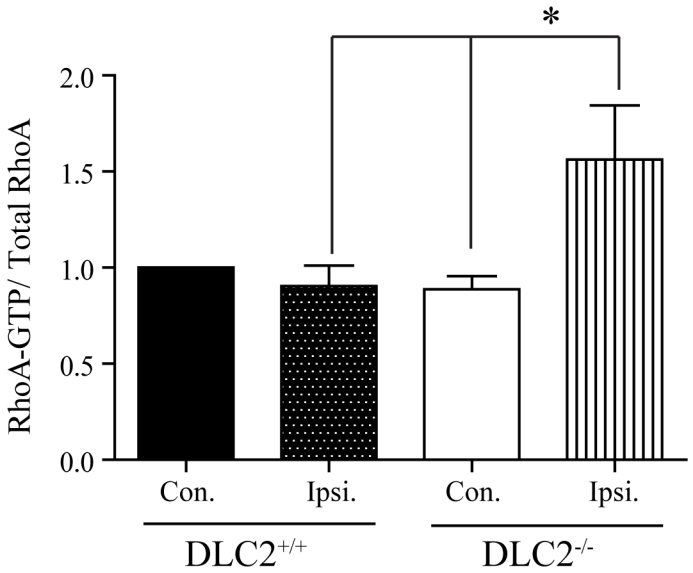
*
RhoA-GTP/ Total RhoA
2.0
1.5
1.0
0.5
0.0
Con.
Ipsi.
Con.
Ipsi.
DLC2+/+
DLC2-/-

Figure 5.

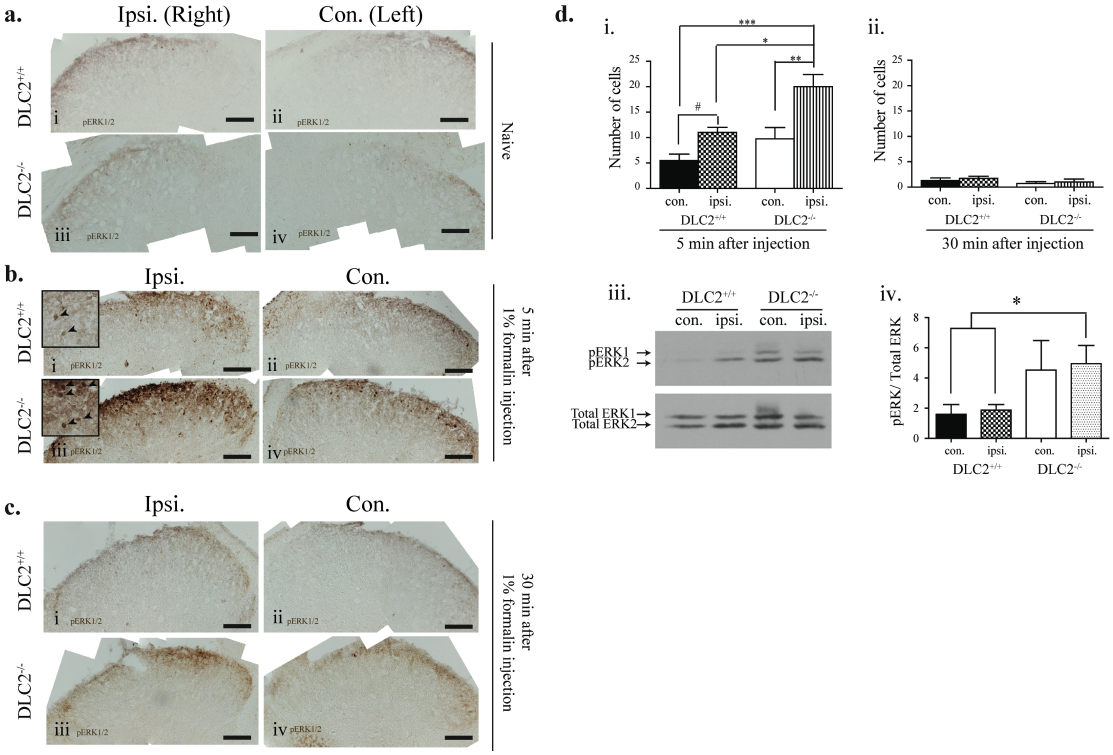
a.
Ipsi. (Right)
Con. (Left)
DLC2+/+
DLC2-/-
i pERK1/2
ii pERK1/2
iii pERK1/2
iv pERK1/2
Naïve
b.
Ipsi.
Con.
5 min after 1% formalin injection
c.
Ipsi.
Con.
30 min after 1% formalin injection
d.
i.
Number of cells
con. ipsi. con. ipsi.
DLC2+/+ DLC2-/-
5 min after injection
ii.
30 min after injection
iii.
pERK1
pERK2
Total ERK1
Total ERK2
iv.
pERK/ Total ERK

Figure 6.

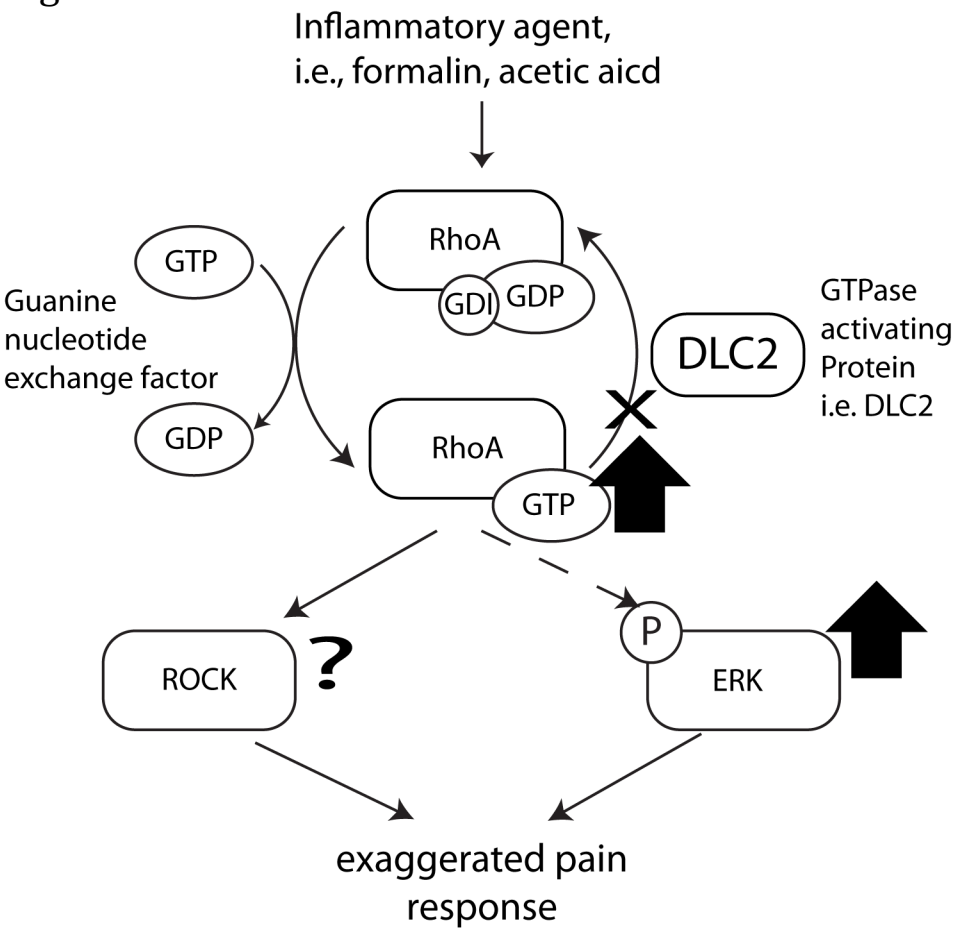
Inflammatory agent,
i.e., formalin, acetic aicd
RhoA
GDI
GDP
GTP
Guanine
nucleotide
exchange factor
GDP
DLC2
GTPase
activating
Protein
i.e. DLC2
RhoA
GTP
ROCK
?
P
ERK
exaggerated pain
response